Discrete Asymptotic Equations for Long Wave Propagation

Article *in* SIAM Journal on Numerical Analysis · January 2016

DOI: 10.1137/15M104325X

Stevan Bellec
University of Bordeaux

Mathieu Colin
Bordeaux INP

Mario Ricchiuto
National Institute for Research in Computer Science and Control

DISCRETE ASYMPTOTIC EQUATIONS FOR LONG WAVE PROPAGATION*

STEVAN BELLEC†, MATHIEU COLIN‡, AND MARIO RICCHIUTO†

Abstract. In this paper, we present a new systematic method to obtain some discrete numerical models for incompressible free-surface flows. The method consists in first discretizing the Euler equations with respect to one variable, keeping the other ones unchanged and then performing an asymptotic analysis on the resulting system. For the sake of simplicity, we choose to illustrate this method in the context of the Peregrine asymptotic regime, that is we propose an alternative numerical scheme for the so-called Peregrine equations. We then study the linear dispersion characteristics of our new scheme and present several numerical experiments to measure the relevance of the method.

Key words. Euler equations, Boussinesq models, Numerical scheme, Finite element method, Asymptotic analysis.

AMS subject classifications. 35Q31, 35Q35, 65M60.

1. Introduction.

Wave transformation in near shore zone is well-described by the incompressible Euler equations. Due to their three-dimensional character, these equations are often too costly if one wants to perform numerical experiments, and often replaced by asymptotic depth-averaged models known as Boussinesq equations. A major characteristic of these models is their ability to describe the dispersive behavior of wave propagation. Generally, the linear and nonlinear dispersion characteristics of the waves represented by Boussinesq models can be improved by including high order contributions in the double asymptotic expansion in terms of the ratios wave height over wave length (dispersion) and wave height over depth (nonlinearity) [18]. Other techniques to improve the linear dispersion characteristics involve the inclusion of extra dispersive differential terms, derived either from a linear wave equation [4, 20], or by replacing depth-averaged values by point values at a properly chosen depth [23]. When numerically simulating the propagation of long waves, the physics represented by these continuous systems of Partial Differential Equations (PDE) is further filtered by the numerical scheme, and in particular by the form of the truncation error. For most of Boussinesq models, the task of designing an accurate numerical discretization is a nontrivial one, due to the presence of dispersion terms. Several approaches exist in literature, each with its own advantages and drawbacks. For details, the interested reader may refer to [8, 9, 13, 16, 22, 25], to the review [10], and references there in. The objective of this paper is to study the interaction scheme-PDE and to propose a framework to obtain new schemes with improved characteristics w.r.t. existing approaches. For this purpose, we introduce a new scheme reversing the model derivation procedure. More precisely, we propose to discretize partially the incompressible Euler equations with respect to one direction using a finite element method, and then follow Peregrine's derivation procedure. This new paradigm leads to a very promising scheme with nice dispersion properties.

The paper is organized as follows. In Section 2 we introduce some notation, the finite element discretization of a well known Boussinesq system, most of the algebraic operators involved and recall our main result. In Section 3, we detail the derivation of the new numerical scheme. The theoretical analysis of these discrete asymptotic models is presented in Section 4. Finally, Section 5 presents a numerical evaluation of the performances of the schemes confirming our theoretical results. The paper is ended by an overlook of future developments related to the new approach

*

†Team CARDAMOM, Inria Bordeaux - Sud-Ouest, (stevan.bellec@inria.fr, mario.ricchiuto@inria.fr).

‡Bordeaux INP, UMR 5251, F-33400,Talence, France, (mathieu.colin@math.u-bordeaux1.fr).

proposed.

2. Setting, notations and main result. Before going further, let us introduce some notations. For simplicity, in this article, we only deal with 2-D and 1-D problems. Denote by (x, z) respectively the horizontal and the vertical spatial dimension. Denote by $d(x)$ the depth at still water and $\eta(t, x)$ the surface elevation from its rest position. The total depth is then $h(t, x) = d(x) + \eta(t, x)$ (see Figure 1).

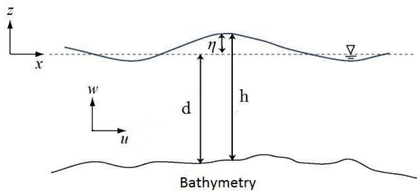

FIGURE 1. *Sketch of the free surface flow problem, main parameters description.*

Let a be a typical wave amplitude, d_0 a reference water depth and λ a typical wavelength. In view of performing an asymptotic analysis, we introduce the nonlinearity parameter ε and the dispersion parameter σ defined by

$$\varepsilon = \frac{a}{d_0},\ \sigma = \frac{d_0}{\lambda}.$$

Under the Boussinesq hypothesis $\varepsilon = \mathcal{O}(\sigma^2)$, Peregrine (see [24]) first derived, from the Euler equations, the following standard system of Boussinesq's type

$$\begin{aligned} &\eta_t + (h\bar{u})_x = 0, \\ &\bar{u}_t + \bar{u}\bar{u}_x + g\eta_x + (\tfrac{d^2}{6}\bar{u}_{txx} - \tfrac{d}{2}(d\bar{u})_{txx}) = 0. \end{aligned} \tag{2.1}$$

The model describes the evolution of the depth-averaged velocity $\bar{u}$ and the surface elevation η within an accuracy of $\mathcal{O}(\varepsilon\sigma^2, \sigma^4)$ w.r.t. the Euler equations. The set of Equations (2.1) is now well-understood from the computation point of view and a classical numerical scheme can be obtained by using the finite element method in the following setting. On an interval $[r, s]$, we introduce a set of nodes

$$r = x_0 < x_1 < \cdots < x_N = s,$$

where, for simplicity, we take a constant space step $\Delta_x = x_{i+1} - x_i$, $\forall i \in \{0, \ldots, N\}$. We denote by E, $\bar{U}$, D and H the vectors of the nodal values of $\eta, \bar{u}$, d and h. Similarly to what has been done in [28, 27] (cf. also [25] and references therein), we apply the $\mathbb{P}_1$ Galerkin method to approximate the variational form of (2.1). In particular, we denote by $\{\varphi_i\}_{0\le i\le N}$ the standard piecewise linear continuous Lagrange basis, and introduce the discrete velocity, wave height and depth polynomials as follows

$$\bar{u}_\Delta(t, x) = \sum_{i=0}^{N} \bar{u}_i(t)\varphi_i(x),\ \eta_\Delta(t, x) = \sum_{i=0}^{N} \eta_i(t)\varphi_i(x),\ d_\Delta(x) = \sum_{i=0}^{N} d_i\varphi_i(x). \tag{2.2}$$

The Galerkin approximation of (2.1), under the hypothesis of exact integration w.r.t. all the discrete polynomials involved, can be written in a compact matrix form

$$\mathcal{M}E_t + \frac{1}{3}\left(2\mathcal{N}(H \diamond \bar{U}) + H \diamond (\mathcal{N}\bar{U}) + \bar{U} \diamond (\mathcal{N}H)\right) = 0, \tag{2.3}$$

$$M\bar{U}_t + \frac{1}{3}\left(\mathcal{N}(\bar{U}^2) + \bar{U} \diamond (\mathcal{N}\bar{U})\right) + g\mathcal{N}E - \frac{1}{6}\{D; \bar{U}_t\} = 0, \tag{2.4}$$

where the matrices $\mathcal{M}$, $\mathcal{N}$ and $\mathcal{Q}$ are the usual mass, derivation, and stiffness matrices arising in the Galerkin discretization and are detailed in [5]. In addition, for given columns vectors $A = (a_i)_{0\leq i\leq N}$ and $B = (b_i)_{0\leq i\leq N}$, we have introduced the operator $\diamond$:

$$\begin{aligned} &\mathbb{R}^N \times \mathbb{R}^N \to \mathbb{R}^N \\ &(A, B) \quad \to A \diamond B := (a_i b_i)_{0\leq i\leq N} \end{aligned}$$

In the sequel, for simplicity A^2 simplifies $A \diamond A$. As an example, the vector $(h_i(\mathcal{N}\bar{U})_i)_{i\in\{1,..,n\}}$ can be rewritten as $H \diamond (\mathcal{N}\bar{U})$. Moreover, for given columns vectors A and B, we set

$$\{A; B\} = \mathcal{Q}(A^2 \diamond B) + A \diamond (\mathcal{Q}(A \diamond B) + 2(A \diamond B) \diamond (\mathcal{Q}A) - B \diamond (\mathcal{Q}A^2).$$

Equations (2.3)-(2.4) will be taken in the sequel as the classical scheme for the Peregrine equations and be used in Sections 4 and 5 to make some comparison with the new scheme introduced in the next section.

The aim of this paper is to propose a systematic method to obtain new numerical models describing free surface flows. It is based on the following idea : reverse the model derivation procedure and *first discretize partially the incompressible Euler equations and then derive fully discrete asymptotic equations by performing an asymptotic analysis.* To illustrate the potential of this idea, we apply this method to the couple Euler-Peregrine equations by applying the Galerkin method to the variable x and then performing the asymptotic analysis of Peregrine's type to the resulting equations. Of course, when one deals with non-linear equations, this procedure does not commute with the classical one. In this paper, for simplicity, we deal with periodic boundary conditions. Note that the adaptation of our strategy with general boundary conditions is a full working that is going to be studied in future. The existence of solutions is not a trivial work even for Dirichlet conditions (see [2]). This strategy is similar to the one proposed for compressible multiphase flows in [1]. As shown in the detailed derivation of the next sections, the new procedure leads to the following discrete equations approximating the discretized Euler system within an accuracy of $\mathcal{O}(\varepsilon\sigma^2, \sigma^4)$

$$\mathcal{M}E_t + \mathcal{M}[H; \bar{U}] = 0, \tag{2.5}$$

$$\mathcal{M}\bar{U}_t + \frac{1}{3}\left(\mathcal{N}(\bar{U}^2) + \bar{U} \diamond (\mathcal{N}\bar{U})\right) + g\mathcal{N}E + \mathcal{M}\left(\frac{D^2}{6} \diamond (\mathcal{K}^2\bar{U}_t) - \frac{D}{2} \diamond (\mathcal{K}[D; \bar{U}_t])\right) = 0, \tag{2.6}$$

having introduced the operator $[\cdot\,;\cdot]$ defined by

$$[A; B] = A \diamond (\mathcal{K}B) + \frac{1}{3}\Big(\mathcal{K}(A \diamond B) - \mathcal{M}^{-1}(A \diamond (\mathcal{N}B)) + 2\mathcal{M}^{-1}(B \diamond (\mathcal{N}A))\Big),$$

with $\mathcal{K} = \mathcal{M}^{-1}\mathcal{N}$. We see that, while involving similar algebraic operations, the new discretization is different from the classical ones, even for a simple case like Peregrine equations. The main differences are found in the treatment of the third order derivatives terms as well as in the nonlinear ones in the continuity (wave height) equation. We will show that scheme (2.6) also converges to an approximation of the Peregrine equations. However, both the linear phase relation, and the linear shoaling gradient provided by (2.5)-(2.6) (see Section 4 and 5) are substantially closer to the exact ones than those given by (2.3)-(2.4). In the sequel, we show how to derive the scheme (2.5)-(2.6) and prove that not only they are consistent with system (2.1), but that they represent a substantial improvement w.r.t. the scheme obtained by discretizing directly the asymptotic equations (2.1).

3. A new setting for deriving discrete asymptotic models.

3.1. Semi-discretization of the 2D-Euler equations in non-dimensional form. The aim of this section is to derive an alternative set of discrete equations, possibly having improved characteristics w.r.t. (2.3)-(2.4), for example a better evaluation of the shoaling gradient phenomenon. For that purpose, we propose to discretize the 2D-Euler equations with respect to one direction, x for example, and then to perform an asymptotic analysis on the resulting equation, similar to the one used to obtain the Peregrine equations (2.1). The Euler equations written in terms of velocity (u, w), pressure p, constant density ρ and vertical gravity acceleration g reads :

$$u_t + uu_x + wu_z + \frac{p_x}{\rho} = 0, \tag{3.1}$$

$$w_t + uw_x + ww_z + \frac{p_z}{\rho} + g = 0, \tag{3.2}$$

$$u_x + w_z = 0, \tag{3.3}$$

$$u_z - w_x = 0, \tag{3.4}$$

where the last equation represents the irrotationality condition. In this paper, since our aim is to obtain a new scheme for the Peregrine system, we restrict ourselves to the 2D version of the Euler equation. We deal with periodic boundary conditions in the x direction, while on the free surface and sea-bed level we use the classical conditions :

- at the free surface $z = \eta$

$$w = \eta_t + u\eta_x,\ p = 0, \tag{3.5}$$

- on the seafloor $z = -d$

$$w = -ud_x. \tag{3.6}$$

Let d_0 be the averaged depth, a a typical wave amplitude, and λ a typical wavelength. The following usual non-dimensional variables are introduced

$$\tilde{x} = \frac{x}{\lambda},\ \tilde{z} = \frac{z}{d_0},\ \tilde{t} = \frac{\sqrt{gd_0}}{\lambda}t,\ \tilde{\eta} = \frac{\eta}{a}, \tilde{u} = \frac{d_0}{a\sqrt{gd_0}}u,\ \tilde{w} = \frac{\lambda}{a}\frac{1}{\sqrt{gd_0}}w,\ \tilde{p} = \frac{p}{gd_0\rho},\ \Delta_{\tilde{x}} = \frac{\Delta_x}{\lambda}.$$

Using the notation introduced above, the Euler equations and the irrotationality condition can be recast in a non-dimensional form as

$$\varepsilon\tilde{u}_{\tilde{t}} + \varepsilon^2\tilde{u}\tilde{u}_{\tilde{x}} + \varepsilon^2\tilde{w}\tilde{u}_{\tilde{z}} + \tilde{p}_{\tilde{x}} = 0, \tag{3.7}$$

$$\varepsilon\sigma^2\tilde{w}_{\tilde{t}} + \varepsilon^2\sigma^2\tilde{u}\tilde{w}_{\tilde{x}} + \varepsilon^2\sigma^2\tilde{w}\tilde{w}_{\tilde{z}} + \tilde{p}_{\tilde{z}} + 1 = 0, \tag{3.8}$$

$$\tilde{u}_{\tilde{x}} + \tilde{w}_{\tilde{z}} = 0, \tag{3.9}$$

$$\tilde{u}_{\tilde{z}} - \sigma^2\tilde{w}_{\tilde{x}} = 0\ \ (\text{so } \tilde{u}_{\tilde{z}} = \mathcal{O}(\sigma^2)), \tag{3.10}$$

The boundary conditions become :

- at the free surface $\tilde{z} = \varepsilon\tilde{\eta}$

$$\tilde{w} = \tilde{\eta}_{\tilde{t}} + \varepsilon\tilde{u}\tilde{\eta}_{\tilde{x}},\ \tilde{p} = 0, \tag{3.11}$$

- at the bed $\tilde{z} = -\tilde{d}$

$$\tilde{w} = -\tilde{u}\tilde{d}_{\tilde{x}}. \tag{3.12}$$

Our goal is to obtain a Boussinesq's type approximation of the Euler system (3.7)-(3.12), under the assumptions $\varepsilon << 1$, $\sigma << 1$, and in the specific regime $\varepsilon = \mathcal{O}(\sigma^2)$, meaning that there exists constant $C > 0$ such that $\varepsilon \leq C\sigma^2$. We now apply a Galerkin method on the variable x keeping t and z unchanged. *It is assumed that $\Delta_{\tilde{x}} = \mathcal{O}(\sigma)$ (it transpires that $\Delta_x = \mathcal{O}(d_0)$).* In the sequel we drop the "˜" and we introduce for all $i \in \{0, ..., N\}$, $u_i(t, z) = u(t, x_i, z)$, $w_i(t, z) = w(t, x_i, z)$, $\eta_i(t, z) = \eta(t, x_i, z)$, $p_i(t, z) = p(t, x_i, z)$. In addition, the discrete horizontal velocity, wave height, depth, vertical velocity and pressure polynomials are written in the Galerkin basis as follows

$$\begin{aligned} &u_\Delta(t,x,z) = \sum_{i=0}^{N} u_i(t,z)\varphi_i(x),\ w_\Delta(t,x,z) = \sum_{i=0}^{N} w_i(t,z)\varphi_i(x),\ \eta_\Delta(t,x) = \sum_{i=0}^{N} \eta_i(t)\varphi_i(x),\\ &p_\Delta(t,x,z) = \sum_{i=0}^{N} p_i(t,z)\varphi_i(x),\ d_\Delta(x) = \sum_{i=0}^{N} d_i\varphi_i(x). \end{aligned} \tag{3.13}$$

We focus on periodic boundary condition that is we introduce $x_{-1} = x_N$ and $x_{N+1} = x_0$. The finite element discrete equations corresponding to (3.7)-(3.8)-(3.9)-(3.10) can be written as, for all $i \in \{0, ..., N\}$

$$\begin{aligned} \varepsilon\frac{\Delta_x}{6}\frac{d}{dt}(u_{i+1} + 4u_i + u_{i-1}) + \frac{\varepsilon^2}{3}\left(\frac{u_{i+1}^2 - u_{i-1}^2}{2} + u_i\frac{u_{i+1} - u_{i-1}}{2}\right) + \frac{p_{i+1} - p_{i-1}}{2}&\\ = -\frac{\varepsilon^2\sigma^2}{3}\left(\frac{w_{i+1}^2 - w_{i-1}^2}{2} + w_i\frac{w_{i+1} - w_{i-1}}{2}\right)&, \end{aligned} \tag{3.14}$$

$$\begin{aligned} \varepsilon\sigma^2\frac{\Delta_x}{6}\frac{d}{dt}(w_{i+1} + 4w_i + w_{i-1}) + \frac{\Delta_x}{6}\frac{d}{dz}(p_{i+1} + 4p_i + p_{i-1}) + \Delta_x&\\ = -\varepsilon^2\sigma^2\big(u_i\frac{w_{i+1} - w_{i-1}}{2} - w_i\frac{u_{i+1} - u_{i-1}}{2}\big)&, \end{aligned} \tag{3.15}$$

$$\frac{u_{i+1} - u_{i-1}}{2} + \frac{\Delta_x}{6}\frac{d}{dz}(w_{i+1} + 4w_i + w_{i-1}) = 0, \tag{3.16}$$

$$\frac{\Delta_x}{6}\frac{d}{dz}(u_{i+1} + 4u_i + u_{i-1}) - \sigma^2\frac{w_{i+1} - w_{i-1}}{2} = 0. \tag{3.17}$$

For the boundary conditions, we propose to integrate (3.11) along the curve $z = \varepsilon\eta$ and equation (3.12) along the curve $z = -d$. For that purpose, we choose to introduce

$$\begin{aligned} &\hat{w}_\Delta = \sum_{i=0}^{N} w_i\big(t, \varepsilon\eta(t,x_i)\big)\varphi_i(x),\ \check{w}_\Delta = \sum_{i=0}^{N} w_i\big(t, -d(x_i)\big)\varphi_i(x),\\ &\hat{u}_\Delta = \sum_{i=0}^{N} u_i\big(t, \varepsilon\eta(t,x_i)\big)\varphi_i(x),\ \check{u}_\Delta = \sum_{i=0}^{N} u_i\big(t, -d(x_i)\big)\varphi_i(x). \end{aligned} \tag{3.18}$$

The boundary conditions (3.11)-(3.12) then write

- at the free surface

$$\frac{\Delta_x}{6}\Big(\hat{w}_{i+1}(t)+4\hat{w}_i(t)+\hat{w}_{i-1}(t)\Big)=\frac{\Delta_x}{6}\frac{d}{dt}\Big(\eta_{i+1}(t)+4\eta_i(t)+\eta_{i-1}(t)\Big)$$
$$+\frac{1}{3}\Big(\frac{\varepsilon\eta_{i+1}(t)\hat{u}_{i+1}(t)-\varepsilon\eta_{i-1}(t)\hat{u}_{i-1}(t)}{2}\tag{3.19}$$
$$-\varepsilon\eta_i(t)\frac{\hat{u}_{i+1}(t)-\hat{u}_{i-1}(t)}{2}+2\hat{u}_i(t)\frac{\varepsilon\eta_{i+1}(t)-\varepsilon\eta_{i-1}(t)}{2}\Big),$$

$$\frac{\Delta_x}{6}\Big(p_{i+1}(t,\varepsilon\eta_{i+1})+4p_i(t,\varepsilon\eta_i)+p_{i-1}(t,\varepsilon\eta_{i-1})\Big)=0,\tag{3.20}$$

- at the bed

$$\frac{\Delta_x}{6}\Big(\check{w}_{i+1}(t)+4\check{w}_i(t)+\check{w}_{i-1}(t)\Big)=$$
$$-\frac{1}{3}\Big(\frac{d_{i+1}\check{u}_{i+1}(t)-d_{i-1}\check{u}_{i-1}(t)}{2}-d_i\frac{\check{u}_{i+1}(t)-\check{u}_{i-1}(t)}{2}+2\check{u}_i(t)\frac{d_{i+1}-d_{i-1}}{2}\Big).\tag{3.21}$$

Introducing the following column vector

$$W=(w_i)_{0\le i\le N},\ U=(u_i)_{0\le i\le N},\ E=(\eta_i)_{0\le i\le N}, P=(p_i)_{0\le i\le N},\ D=(d_i)_{0\le i\le N},\ \mathcal{I}=\begin{pmatrix}1\\ \vdots\\ 1\end{pmatrix}$$
$$\hat{W}=\Big(w_i(\varepsilon\eta_i)\Big)_{0\le i\le N},\ \hat{U}=\Big(u_i(\varepsilon\eta_i)\Big)_{0\le i\le N},\ \check{W}=\Big(w_i(-d_i)\Big)_{0\le i\le N},\ \check{U}=\Big(u_i(-d_i)\Big)_{0\le i\le N},$$

we can rewrite Equations (3.14)-(3.21) into the following matrix-form :

$$\varepsilon\frac{d}{dt}\mathcal{M}U+\frac{\varepsilon^2}{3}\left(\mathcal{N}(U^2)+U\diamond(\mathcal{N}U)\right)+\mathcal{N}P=-\frac{\varepsilon^2\sigma^2}{3}\left(\mathcal{N}(W^2)+W\diamond(\mathcal{N}W)\right),\tag{3.22}$$

$$\varepsilon\sigma^2\frac{d}{dt}\mathcal{M}W+\frac{d}{dz}\mathcal{M}P+\mathcal{I}=-\varepsilon^2\sigma^2\left(U\diamond(\mathcal{N}W)-W\diamond(\mathcal{N}U)\right),\tag{3.23}$$

$$\mathcal{N}U+\mathcal{M}\frac{d}{dz}W=0,\tag{3.24}$$

$$\mathcal{M}\frac{d}{dz}U-\sigma^2\mathcal{N}W=0.\tag{3.25}$$

The boundary conditions become

- at the free surface

$$\mathcal{M}\hat{W}=\frac{d}{dt}\mathcal{M}E+\frac{\varepsilon}{3}\Big(\mathcal{N}(E\diamond\hat{U})-E\diamond(\mathcal{N}\hat{U})+2\hat{U}\diamond(\mathcal{N}E)\Big),\ \mathcal{M}\hat{P}=0,\tag{3.26}$$

- at the bottom

$$\mathcal{M}\check{W}=-\frac{1}{3}\Big(\mathcal{N}(D\diamond\check{U})-D\diamond(\mathcal{N}\check{U})+2\check{U}\diamond(\mathcal{N}D)\Big).\tag{3.27}$$

System (3.22)-(3.27) represents the first step in our analysis. The next two sections are dedicated to the transformation of this system into an asymptotic set of equations.

3.2. Asymptotic expansions on the velocity U and the pressure p. In this section, we derive an asymptotic expansion in terms of σ for the semi-discrete horizontal velocity $U = U(t,z)$ following the procedure presented by Peregrine in [24]. More precisely, we prove the following proposition.

PROPOSITION 1 (Consistency results). *The pressure P and the velocity U satisfy expansion of the form*

$$P = \varepsilon E - z\mathcal{I} + \varepsilon\sigma^2 \left(\frac{z^2}{2}\mathcal{K}U^0 + z[D;U^0]\right) + \mathcal{O}(\varepsilon^2\sigma^2, \varepsilon\sigma^4)$$

$$U = \bar{U} + \sigma^2 \left(\frac{D^2}{6} \diamond (\mathcal{K}^2\bar{U}) - \frac{z^2}{2}\mathcal{K}^2\bar{U} - z\mathcal{K}[D;\bar{U}] - \frac{D}{2} \diamond (\mathcal{K}[D;\bar{U}])\right) + \mathcal{O}(\varepsilon\sigma^2, \sigma^4),$$

where the averaged velocity is defined in (3.36).

Proof. Since $\mathcal{M}$ is invertible, we obtain from the integration of (3.25) between 0 and an arbitrary depth z,

$$U(t,z) = U^0(t) + \mathcal{O}(\sigma^2), \tag{3.28}$$

where $U^0(t)$ is a constant depending only on t and corresponds to the value of U at $z = 0$. Substituting relation (3.28) in equation (3.24) and setting $\mathcal{K} = \mathcal{M}^{-1}\mathcal{N}$, we derive

$$\frac{d}{dz}W = -\mathcal{K}U^0 + \mathcal{O}(\sigma^2). \tag{3.29}$$

Integrating each line $i \in \{0, ..., N\}$ of equation (3.29) with respect to z between $-d_i$ and an arbitrary depth z ($-d_i < z < \epsilon\eta_i$), using the boundary condition (3.27) and the estimates (3.28) on U, we obtain

$$W = -(z\mathcal{I}+D)\diamond(\mathcal{K}U^0) - \frac{1}{3}\Big(\mathcal{K}(D\diamond U^0) - \mathcal{M}^{-1}(D\diamond(\mathcal{N}U^0)) + 2\mathcal{M}^{-1}(U^0\diamond(\mathcal{N}D))\Big) + \mathcal{O}(\sigma^2). \tag{3.30}$$

In view of (3.30), it is natural to introduce the following bracket

$$[A;B] = A \diamond (\mathcal{K}B) + \frac{1}{3}\left(\mathcal{K}(A \diamond B) - \mathcal{M}^{-1}(A \diamond (\mathcal{N}B)) + 2\mathcal{M}^{-1}(B \diamond (\mathcal{N}A))\right). \tag{3.31}$$

Plugging (3.30) in (3.25) and integrating the resulting equation between 0 and z, one derives the following expansion on U

$$U = U^0 - \sigma^2\left(\frac{z^2}{2}\mathcal{K}^2U^0 + z[D;U^0]\right) + \mathcal{O}(\sigma^4). \tag{3.32}$$

Looking for a similar expansion on the pressure array P, we substitute Equation (3.30) in Equation (3.23).Using the fact that $\mathcal{M}\mathcal{I} = \mathcal{I}$, we obtain

$$\frac{d}{dz}P = -\mathcal{I} - \varepsilon\sigma^2\frac{d}{dt}\left(z\mathcal{K}U^0 + [D;U^0]\right) + \mathcal{O}(\varepsilon^2\sigma^2, \varepsilon\sigma^4). \tag{3.33}$$

Furthermore, integrating each line $i \in \{0, ..., N\}$ of equation (3.33) with respect to z from an arbitrary depth to the free surface $\varepsilon\eta_i$, we can write

$$P = \varepsilon E - z\mathcal{I} + \varepsilon\sigma^2 \left(\frac{z^2}{2}\mathcal{K}U^0 + z[D;U^0]\right) + \mathcal{O}(\varepsilon^2\sigma^2, \varepsilon\sigma^4) \tag{3.34}$$

Substituting equations (3.34) and (3.32) in (3.22), we obtain an equation for the zero-th order velocity U^0, equivalent to Equation 2.28 in [27], which reads :

$$\frac{d}{dt}\mathcal{M}U^0 + \frac{\varepsilon}{3}\left(\mathcal{N}(U^0 \diamond U^0) + U^0 \diamond (\mathcal{N}U^0)\right) + \mathcal{N}E = \mathcal{O}(\varepsilon\sigma^2, \sigma^4). \tag{3.35}$$

Note that the choice of the constant of integration in (3.28) is not unique. However it transpires that the choice of U^0 (which is the value of the horizontal velocity U at $z = 0$) is not optimal as observed in [27]. This is why, in the sequel, we are going to get rid of it by introducing the averaged velocity matrix $\bar{U} = (\bar{u}_i)_{0\leq i\leq N}$ where

$$\bar{u}_i = \frac{1}{d_i + \varepsilon\eta_i}\int_{-d_i}^{\varepsilon\eta_i} u_i dz, \tag{3.36}$$

and by looking for the equation satisfied by $\bar{U}$. In this direction, we first derive the relation between U_0 and $\bar{U}$. Equation (3.32) provides, for all $i \in \{0, ..., N\}$,

$$u_i = u_i^0 - \sigma^2\left(\frac{z^2}{2}\left(\mathcal{K}^2U^0\right)_i + z\left(\mathcal{K}[D;U^0]\right)_i\right) + \mathcal{O}(\sigma^4),$$

and by integration between $-d_i$ and $\varepsilon\eta_i$, we immediately get, using Taylor expansion,

$$\begin{aligned}
\bar{u}_i &= u_i^0 - \frac{\sigma^2}{\varepsilon\eta_i + d_i}\left(\int_{-d_i}^{\varepsilon\eta_i}\frac{z^2}{2}dz\left(\mathcal{K}^2U^0\right)_i + \int_{-d_i}^{\varepsilon\eta_i} zdz\left(\mathcal{K}[D;U^0]\right)_i\right) + \mathcal{O}(\sigma^4),\\
&= u_i^0 - \frac{\sigma^2}{(d_i + \varepsilon\eta_i)}\left(\frac{d_i^3}{6}\left(\mathcal{K}^2U^0\right)_i - \frac{d_i^2}{2}\left(\mathcal{K}[D;U^0]\right)_i\right) + \mathcal{O}(\varepsilon\sigma^2, \sigma^4),\\
&= u_i^0 - \sigma^2\left(\frac{d_i^2}{6}\left(\mathcal{K}^2U^0\right)_i - \frac{d_i}{2}\left(\mathcal{K}[D;U^0]\right)_i\right) + \mathcal{O}(\varepsilon\sigma^2, \sigma^4).
\end{aligned}$$

This furnishes the desired relation

$$\bar{U} = U^0 - \sigma^2\left(\frac{D^2}{6}\diamond(\mathcal{K}^2U^0) - \frac{D}{2}\diamond(\mathcal{K}[D;U^0])\right) + \mathcal{O}(\varepsilon\sigma^2, \sigma^4), \tag{3.37}$$

or equivalently

$$U^0 = \bar{U} + \sigma^2\left(\frac{D^2}{6}\diamond(\mathcal{K}^2U^0) - \frac{D}{2}\diamond(\mathcal{K}[D;U^0])\right) + \mathcal{O}(\varepsilon\sigma^2, \sigma^4). \tag{3.38}$$

Then it transpires that $U^0 = \bar{U} + \mathcal{O}(\varepsilon, \sigma^2)$. Substituting in (3.38), we derive

$$U^0 = \bar{U} + \sigma^2\left(\frac{D^2}{6}\diamond(\mathcal{K}^2\bar{U}) - \frac{D}{2}\diamond(\mathcal{K}[D;\bar{U}])\right) + \mathcal{O}(\varepsilon\sigma^2, \sigma^4). \tag{3.39}$$

Finally, plugging (3.39) into (3.32), one obtains the expansion of U as a function of the depth averaged velocity $\bar{U}$

$$U = \bar{U} + \sigma^2\left(\frac{D^2}{6}\diamond(\mathcal{K}^2\bar{U}) - \frac{z^2}{2}\mathcal{K}^2\bar{U} - z\mathcal{K}[D;\bar{U}] - \frac{D}{2}\diamond(\mathcal{K}[D;\bar{U}])\right) + \mathcal{O}(\varepsilon\sigma^2, \sigma^4). \tag{3.40}$$

3.3. Depth-averaged equations. The aim of this section is to provide the final new discrete numerical model of Peregrine's type. In order to derive the equation on $\bar{U}$ (known as the momentum equation in the literature), we substitute (3.39) in (3.35) to obtain :

$$\frac{d}{dt}\mathcal{M}\bar{U} + \frac{\varepsilon}{3}\left(\mathcal{N}(\bar{U}^2) + \bar{U}\diamond(\mathcal{N}\bar{U})\right) + \mathcal{N}E + \sigma^2\mathcal{M}\frac{d}{dt}\left(\frac{D^2}{6}\diamond(\mathcal{K}^2\bar{U}) - \frac{D}{2}\diamond\mathcal{K}[D;\bar{U}]\right) = \mathcal{O}(\varepsilon\sigma^2,\sigma^4)$$

In addition, to derive an equation on E (that is the continuity equation), we combine (3.26) and (3.27) to get

$$\begin{aligned}\hat{W} - \check{W} = {} & \frac{d}{dt}E + \varepsilon\frac{\mathcal{M}^{-1}}{3}(\mathcal{N}(E\diamond\hat{U}) - E\diamond(\mathcal{N}\hat{U}) + 2\hat{U}\diamond(\mathcal{N}E)) \\ & + \frac{\mathcal{M}^{-1}}{3}(\mathcal{N}(D\diamond\check{U}) - D\diamond(\mathcal{N}\check{U}) + 2\check{U}\diamond(\mathcal{N}D)).\end{aligned} \tag{3.41}$$

We integrate each lines of (3.41) between $-d_i$ and $\varepsilon\eta_i$, for all $i\in\{0,...,N\}$, to obtain

$$\int_{-d_i}^{\varepsilon\eta_i}(\mathcal{K}U)_i dz + \hat{W}_i - \check{W}_i = 0,$$

which can be recast as

$$E_t + [H;\bar{U}] + B = 0, \tag{3.42}$$

where

$$\begin{aligned}B = {} & \left(\int_{-d_i}^{\varepsilon\eta_i}(\mathcal{K}U)_i dz\right)_{0\le i\le N} - [H;\bar{U}] + \frac{\varepsilon}{3}(\mathcal{K}(E\diamond\hat{U}) - \mathcal{M}^{-1}(E\diamond(\mathcal{N}\hat{U})) + 2\mathcal{M}^{-1}(\hat{U}\diamond(\mathcal{N}E))) \\ & -\frac{1}{3}(\mathcal{K}(-D\diamond\check{U}) - \mathcal{M}^{-1}(-D\diamond(\mathcal{N}\check{U})) + 2\mathcal{M}^{-1}(\check{U}\diamond(\mathcal{N}(-D))).\end{aligned} \tag{3.43}$$

We can remark that the expression B is no more than a discretized version of the so-called Leibniz' Rule[1]. As a consequence, it transpires that B has the same accuracy of order $\mathcal{O}(\varepsilon\sigma^2,\sigma^4)$ than that of the equations and then can be neglected in the sequel. In order to be more precise, we compute explicitly B by taking successively $z=\varepsilon\eta_i$ and $z=-d_i$ in (3.40) to obtain the values of $\hat{U}$ and $\check{U}$:

$$\begin{aligned}\hat{U} = {} & \bar{U} + \sigma^2\left(\frac{D^2}{6}\diamond(\mathcal{K}^2\bar{U}) - \frac{\varepsilon^2E^2}{2}\mathcal{K}^2\bar{U} - \varepsilon E\diamond\mathcal{K}[D;\bar{U}] - \frac{D}{2}\diamond(\mathcal{K}[D;\bar{U}])\right) + \mathcal{O}(\varepsilon\sigma^2,\sigma^4) \\ \check{U} = {} & \bar{U} + \sigma^2\left(-\frac{D^2}{3}\diamond(\mathcal{K}^2\bar{U}) + \frac{D}{2}\diamond(\mathcal{K}[D;\bar{U}])\right) + \mathcal{O}(\varepsilon\sigma^2,\sigma^4).\end{aligned} \tag{3.44}$$

[1]We recall the Leibniz' Rule : Given $f(x,z), a(x)$ and $b(x)$, where f and $\frac{\partial f}{\partial x}$ are continuous in x and z, and a and b are differentiable functions of x,

$$\frac{\partial}{\partial x}\left(\int_{a(x)}^{b(x)} f(x,z)dz\right) = \int_{a(x)}^{b(x)}\frac{\partial}{\partial x}f(x,z)dz + f(x,b(x))b'(x) - f(x,a(x))a'(x).$$

By substituting Equations (3.40) and (3.44) into Equation (3.43), this provides the complete expression of B

$$B = \sigma^2\Bigg(\frac{1}{6}D\diamond(\mathcal{K}(D^2\diamond(\mathcal{K}^2\bar{U}))) - \frac{1}{6}D^3\diamond(\mathcal{K}^3\bar{U}) - \frac{1}{9}\mathcal{K}(D^3\diamond(\mathcal{K}^2\bar{U}))$$
$$+\frac{1}{9}\mathcal{M}^{-1}D\diamond(\mathcal{N}(D^2\diamond(\mathcal{K}^2\bar{U}))) + \frac{1}{2}D^2\diamond(\mathcal{K}^2[D;\bar{U}]) - \frac{1}{2}D\diamond(\mathcal{K}(D\diamond(\mathcal{K}[D;\bar{U}])))$$
$$+\frac{1}{6}\mathcal{K}(D^2\diamond(\mathcal{K}[D;\bar{U}])) - \frac{1}{6}\mathcal{M}^{-1}D\diamond(\mathcal{N}D\diamond(\mathcal{K}[D;\bar{U}]))$$
$$-\frac{2}{9}\mathcal{M}^{-1}(\mathcal{N}D)\diamond(D^2\diamond(\mathcal{K}^2\bar{U})) + \frac{1}{3}\mathcal{M}^{-1}((\mathcal{N}D)\diamond(D\diamond(\mathcal{K}[D;\bar{U}])))\Bigg) + \mathcal{O}(\varepsilon\sigma^2,\sigma^4).$$

Finally, our new non-dimensionalized system reads (note that we have multiply (3.42) by $\mathcal{M}$)

$$\frac{d}{dt}\mathcal{M}E + \mathcal{M}[H;\bar{U}] + \mathcal{M}B = 0. \tag{3.45}$$

$$\frac{d}{dt}\mathcal{M}\bar{U} + \frac{\varepsilon}{3}\left(\mathcal{N}(\bar{U}^2) + \bar{U}\diamond(\mathcal{N}\bar{U})\right) + \mathcal{N}E + \sigma^2\mathcal{M}\frac{d}{dt}\left(\frac{D^2}{6}\diamond(\mathcal{K}^2\bar{U}) - \frac{D}{2}\diamond\mathcal{K}[D;\bar{U}]\right) = \mathcal{O}(\varepsilon\sigma^2,\sigma^4) \tag{3.46}$$

To go further, we now investigate the behavior of the vector B by establishing the following proposition.

Proposition 2 (Consistency results). *For any bathymetry d, the additional term B in Equation (3.45) satisfies*

$$B = \mathcal{O}(\varepsilon\sigma^2,\sigma^4).$$

As a consequence, the numerical scheme (3.45)-(3.46) becomes

$$\frac{d}{dt}\mathcal{M}E + \mathcal{M}[H;\bar{U}] = \mathcal{O}(\varepsilon\sigma^2,\sigma^4), \tag{3.47}$$

$$\frac{d}{dt}\mathcal{M}\bar{U} + \frac{1}{3}\left(\mathcal{N}(\bar{U}^2) + \bar{U}\diamond(\mathcal{N}\bar{U})\right) + \mathcal{N}E - \sigma^2\frac{d}{dt}\left(\frac{d_0^2}{3}(\mathcal{N}\mathcal{K}\bar{U})\right) = \mathcal{O}(\varepsilon\sigma^2,\sigma^4), \tag{3.48}$$

and is consistent with the Peregrine Equations (2.1).

Proof. For a better understanding, we first assume that the bathymetry $d = d_0$ is constant. In this setting, one has $D = d_0\mathcal{I}$ and the operator $D\diamond$ is no more than the multiplication by the real d_0, that is, for example, $D\diamond U = d_0 U$. Hence B is equal to

$$B = 0 + \mathcal{O}(\varepsilon\sigma^2,\sigma^4).$$

More generally, assume now that the bathymetry d is not constant. For any regular function u and its discrete version $(u_i)_{0\le i\le N}$, a Taylor expansion provides

$$u_{i+1} = u_i + \Delta_x u_x(x_i) + \frac{\Delta_x^2}{2}u_{xx}(x_i) + \frac{\Delta_x^3}{6}u_{xxx}(x_i) + ..., \tag{3.49}$$

and

$$u_{i-1} = u_i - \Delta_x u_x(x_i) + \frac{\Delta_x^2}{2}u_{xx}(x_i) - \frac{\Delta_x^3}{6}u_{xxx}(x_i) + ... \tag{3.50}$$

Combining (3.49) and (3.50), we can prove that, for all $i \in \{0, ..., N\}$

$$(\mathcal{N}U)_i = u_x(x_i) + \frac{\Delta_x^2}{6} u_{xxx}(x_i) + \mathcal{O}(\Delta_x^4),$$

$$(\mathcal{M}^{-1}U)_i = u(x_i) - \frac{\Delta_x^2}{6} u_{xx}(x_i) + \mathcal{O}(\Delta_x^4),\ (\mathcal{K}U)_i = u_x(x_i) + \mathcal{O}(\Delta_x^4).$$

Plugging these expansions in Equations (3.45) and (3.46), we obtain

$$\begin{aligned}\eta_t + (h\bar{u})_x - \frac{\Delta_x^2}{6}\Bigg(&\eta_{txx} + (h\bar{u})_{xxx} + h_{xx}\bar{u}_x + \sigma^2\Big(\frac{d^2 d_{xx}\bar{u}_{xxx}}{6} + \frac{7}{6} d d_x d_{xx} \bar{u}_{xx} \\ &+ \big(\frac{3}{2} d d_{xx}^2 d_x^2 d_{xx} + \frac{5}{6} d d_x d_{xxx}\big)\bar{u}_x + d d_{xx} d_{xxx} \bar{u}\Big)\Bigg) + \mathcal{O}(\Delta_x^4) = \mathcal{O}(\varepsilon\sigma^2, \sigma^4),\end{aligned}$$

$$\begin{aligned}\bar{u}_t + \bar{u}\bar{u}_x + \eta_x + \sigma^2\left(\frac{d^2}{6}\bar{u}_{txx} - \frac{d}{2}(d\bar{u})_{txx}\right) + \frac{\Delta_x^2}{6}\Bigg(\bigg(&\bar{u}_t + \bar{u}\bar{u}_x + \eta_x + \sigma^2 \frac{d^2}{6}\bar{u}_{txx} \\ -\sigma^2 \frac{d}{2}(d\bar{u})_{txx}\bigg)_{xx} - \bar{u}_x\bar{u}_{xx} + \sigma^2\frac{d}{2}(d_{xx}\bar{u}_x)_x\Bigg) &+ \mathcal{O}(\Delta_x^4) = \mathcal{O}(\varepsilon\sigma^2, \sigma^4),\end{aligned}$$

proving that our numerical scheme is consistent with the continuous Peregrine equations(2.1). In addition, B is equal to

$$\begin{aligned}B = -\,\sigma^2 \frac{\Delta_x^2}{6}\Bigg(&\frac{d^2 d_{xx}\bar{u}_{xxx}}{6} + \frac{7}{6} d d_x d_{xx}\bar{u}_{xx} + \big(\frac{3}{2} d d_{xx}^2 d_x^2 d_{xx} + \frac{5}{6} d d_x d_{xxx}\big)\bar{u}_x \\ &+ d d_{xx} d_{xxx}\bar{u} + \mathcal{O}(\Delta_x^2)\Bigg) + \mathcal{O}(\varepsilon\sigma^2, \sigma^4),\end{aligned}$$

from which it transpires that B contains only terms of order $\Delta_x^2\sigma^2$, $\varepsilon\sigma^2$ or σ^4 (actually, B is consistent with Leibniz' Rule). Recalling that $\Delta_{\tilde{x}} = \mathcal{O}(\sigma)$, one has

$$B = \sigma^2 \mathcal{O}(\Delta_{\tilde{x}}^2) + \mathcal{O}(\varepsilon\sigma^2, \sigma^4) = \mathcal{O}(\varepsilon\sigma^2, \sigma^4),$$

which ends the proof of Proposition 2. ∎

To end this section, we return to the physical variables and neglect the contribution of B in (3.45)-(3.46) to obtain our new numerical scheme for the Peregrine Equations (2.1)

$$\frac{d}{dt}\mathcal{M}E + \mathcal{M}[H; \bar{U}] = 0, \tag{3.51}$$

$$\frac{d}{dt}\mathcal{M}\bar{U} + \frac{1}{3}\left(\mathcal{N}(\bar{U}^2) + \bar{U} \diamond (\mathcal{N}\bar{U})\right) + g\mathcal{N}E + \mathcal{M}\frac{d}{dt}\left(\frac{D^2}{6} \diamond (\mathcal{K}^2\bar{U}) - \frac{D}{2} \diamond (\mathcal{K}[D; \bar{U}])\right) = 0. \tag{3.52}$$

4. Study of the linear dispersion characteristics. The aim of this section is to give some insights to measure the accuracy of the new method developped in the previous sections. For that purpose, we exhibit the dispersion relation as well as the shoaling coefficients of the linearized version of the scheme (3.51)-(3.52). This study is widely inspired by the one proposed by Dingemans in [11] in the context of slowly-varying water depth, that is we assume that $d = d(\beta x)$ with $\beta << 1$. For the sake of completness, we also compare our computations with the ones performed on the linearized version of the classical scheme (2.3)-(2.4).

4.1. Linear characteristics of the new numerical model. We first introduce the linearized version of the scheme (3.51)-(3.52) around the rest state which reads

$$\frac{d}{dt}\mathcal{M}E + \mathcal{M}[D;\bar{U}] = 0, \tag{4.1}$$

$$\frac{d}{dt}\mathcal{M}\bar{U} + g\mathcal{N}E + \mathcal{M}\frac{d}{dt}\left(\frac{D^2}{6}\diamond(\mathcal{K}^2\bar{U}) - \frac{D}{2}\diamond(\mathcal{K}[D;\bar{U}])\right) = 0. \tag{4.2}$$

As usual, when one deals with linear equations, a lot of computations can be performed explicitly. Indeed, differentiating (4.2) with respect to t, multiplying (4.1) by $\mathcal{N}$ and substituting the resulting equations, one obtains a decouple equation on the vector $\bar{U}$:

$$\mathcal{M}\bar{U}_{tt} - g\mathcal{N}[D;\bar{U}] + \mathcal{M}\left(\frac{D^2}{6}\diamond(\mathcal{K}^2\bar{U}) - \frac{D}{2}\diamond(\mathcal{K}[D;\bar{U}])\right)_{tt} = 0. \tag{4.3}$$

In order to exhibit the dispersion relation associated with (4.1)-(4.2), we then look for a *plane-wave* solution under the form $\bar{U} = \left(\bar{u}_i\right)_{0\leq i\leq N}$, where

$$\bar{u}_i = \bar{u}(t,x_i) \text{ with } \bar{u}(t,x) = \mathbf{U}(\beta x)\exp\left(-j\omega t + \frac{j}{\beta}K(\beta x)\right),\ j^2 = -1. \tag{4.4}$$

Owning the solution $\bar{U}$, it is pertinent to introduce the wave number $k(\beta x) = \frac{\partial}{\partial x}\left(\frac{1}{\beta}K(\beta x)\right)$, and for all $i = 0,...,N$, $k_i = k(\beta x_i)$. Then, we determine conditions on k and $\mathbf{U}$ so that $\bar{U}$ is a solution to the linear system (4.3). A Taylor expansion around the point $x = x_i$ provides directly

$$\bar{u}_{i+1} = \left(1 + \beta(j\frac{\Delta_x^2}{2}k'(\beta x_i) + \Delta_x\frac{\mathbf{U}'(\beta x_i)}{\mathbf{U}_i})\right)\bar{u}_i e^{jk_i\Delta_x} + \mathcal{O}(\beta^2), \tag{4.5}$$

$$\bar{u}_{i-1} = \left(1 + \beta(j\frac{\Delta_x^2}{2}k'(\beta x_i) - \Delta_x\frac{\mathbf{U}'(\beta x_i)}{\mathbf{U}_i})\right)\bar{u}_i e^{-jk_i\Delta_x} + \mathcal{O}(\beta^2). \tag{4.6}$$

In view of (4.3), we deduce that, $\forall i \in \{1,..,n\}$

$$(\mathcal{N}\bar{U})_i = \left(jk_i\text{sinc}(k_i\Delta_x) - \beta\frac{k_i^2\Delta_x^2}{2}\text{sinc}(k_i\Delta_x)\frac{k'(\beta x_i)}{k_i} + \beta\cos(k_i\Delta_x)\frac{\mathbf{U}'(\beta x_i)}{\mathbf{U}_i}\right)\bar{u}_i + \mathcal{O}(\beta^2). \tag{4.7}$$

$$(\mathcal{M}\bar{U})_i = \left(\frac{1}{3}(2+\cos(k_i\Delta_x)) + j\beta\frac{k_i\Delta_x^2}{6}(\cos(k_i\Delta_x)\frac{k'(\beta x_i)}{k_i} + 2\text{sinc}(k_i\Delta_x)\frac{\mathbf{U}'(\beta x_i)}{\mathbf{U}_i})\right)\bar{u}_i + \mathcal{O}(\beta^2). \tag{4.8}$$

Note that it is not possible to plug directly (4.7)-(4.8) into (4.3), due to the presence of the vector $(\mathcal{M}^{-1}\bar{U})$ in the bracket $[D;\bar{U}]$. Indeed, it is necessary to express each term $(\mathcal{M}^{-1}\bar{U})$ with respect to $\bar{u}_i$. To overcome this difficulty, the idea is to introduce the following new variables :

$$V = \mathcal{M}^{-1}\mathcal{N}\left(D\diamond\bar{U}\right),\ X = \mathcal{M}^{-1}\mathcal{N}\bar{U},\ Z = \mathcal{M}^{-1}\left(D\diamond(\mathcal{N}\bar{U})\right),\ W = \mathcal{M}^{-1}(\bar{U}\diamond(\mathcal{N}D)),$$
$$Y = \mathcal{M}^{-1}\mathcal{N}X,\ T = \left(D\diamond X + \frac{1}{3}(V - Z + 2W)\right),\ S = \mathcal{M}^{-1}\mathcal{N}T.$$

To perform asymptotic expansions of order β^2 on these variables. Using these new vectors, one can rewrite Equation (4.3) into

$$\mathcal{M}\bar{U}_{tt} - g\mathcal{N}T + \mathcal{M}\left(\frac{D^2}{6}\diamond Y_{tt} - \frac{D}{2}\diamond S_{tt}\right) = 0 \tag{4.9}$$

Note first that the vectors V, X, Z, W, Y and T depends only on $\bar{U}$. It is then natural to introduce the following exponential functions (in the same form than $\bar{u}$) $\mathbf{v}$, $\mathbf{x}$, $\mathbf{z}$, $\mathbf{w}$, $\mathbf{y}$,$\mathbf{t}$ and $\mathbf{s}$ where $\mathbf{V}(\beta x)$, $\mathbf{X}(\beta x)$, $\mathbf{Z}(\beta x)$, $\mathbf{W}(\beta x)$, $\mathbf{Y}(\beta x)$, $\mathbf{T}(\beta x)$ and $\mathbf{S}(\beta x)$ denote the amplitude of functions.It is possible to express these amplitude in function of $\mathbf{U}$ performing an asymptotic analysis with respect to the parameter β (see [5] for details).

Using Equations (4.7) and (4.8) and these expansions, one can rewrite (4.9) for all $i \in \{1, .., n\}$. Collecting in the resulting equation the term of order β^0, one obtains the expression of ω, for all $i = 0, ..., N$,

$$\frac{\omega^2}{gd_ik_i^2} = \frac{\operatorname{sinc}(k_i\Delta_x)^2}{(\frac{1}{3}(2+\cos(k_i\Delta_x)))^2 + \frac{k_i^2d_i^2}{3}\operatorname{sinc}(k_i\Delta_x)^2}. \tag{4.10}$$

Furthermore, collecting the term of order β, one obtains a relation between $\mathbf{U}$, k, and the bathymetry d :

$$\alpha_{1,i}^{(1)}\frac{\mathbf{U}'(\beta x_i)}{\mathbf{U}_i} + \alpha_{2,i}^{(1)}\frac{d'(\beta x_i)}{d_i} + \alpha_{3,i}^{(1)}\frac{k'(\beta x_i)}{k_i} = 0. \tag{4.11}$$

Equation (4.11) describes the effect of linear shoaling since the numbers $\alpha_{1,i}^{(1)}$, $\alpha_{2,i}^{(1)}$ and $\alpha_{3,i}^{(1)}$ are known as the linear shoaling coefficients. Using (4.10), one can compute these three coefficients (we omit the details for simplicity). Differentiating formally the dispersion relation (4.10) and assuming that ω is constant, we deduce that k_i has to satisfy the following condition

$$\frac{k'(\beta x_i)}{k_i} = -\alpha_4^{(1)}\frac{d'(\beta x_i)}{d_i}, \tag{4.12}$$

This relation is used to compute formally k_i for $i = 0, ..., N$ and for a given bathymetry and therefore to obtain the coefficients $\alpha_{1,i}^{(1)}$, $\alpha_{2,i}^{(1)}$ and $\alpha_{3,i}^{(1)}$. Finally, following [11], we obtain an expression of the amplitude velocity $\mathbf{U}_i$, for all $i = 0, ..., N$

$$\frac{\mathbf{U}_i'}{\mathbf{U}_i} = -\alpha_{s,i}^{(1)}\frac{d_i'}{d_i}, \quad \text{where } \alpha_{s,i}^{(1)} = \frac{\alpha_{2,i}^{(1)} - \alpha_{3,i}^{(1)}\alpha_{4,i}^{(1)}}{\alpha_{1,i}^{(1)}}. \tag{4.13}$$

In order to find the theoretical amplitude of the surface elevation $\mathbf{A}$, we assume that $E = (\eta_i)_{0\le i\le N}$, where $\eta_i = \mathbf{A}(\beta x_i)\exp\left(-j\omega t + \frac{j}{\beta}K(\beta x_i)\right)$. Substituting in Equation (4.1), we obtain an expression of $\mathbf{A}_i$ in function of $\mathbf{U}_i$ for all $i = 0, ..., N$

$$\mathbf{A}_i = \frac{d_i}{\sqrt{gd_i}}\sqrt{1 + \frac{k_i^2d_i^2}{3}\frac{\operatorname{sinc}(k_i\Delta_x)}{\frac{1}{3}(2+\cos(k_i\Delta_x))}}\mathbf{U}_i. \tag{4.14}$$

4.2. Linear characteristics of the classical Peregrine model. We consider now the linear classical numerical model presented in Section 3.

$$\mathcal{M}\frac{d}{dt}E + \frac{1}{3}\left(2\mathcal{N}(D \diamond \bar{U}) + D \diamond (\mathcal{N}\bar{U}) + \bar{U} \diamond (\mathcal{N}D)\right) = 0, \tag{4.15}$$

$$\frac{d}{dt}\mathcal{M}\bar{U} + g\mathcal{N}E - \frac{1}{6}\{D; \bar{U}_t\} = 0, \tag{4.16}$$

We reproduce the same procedure as in Section 4.1. The terms of order of β^0 gives the linear dispersion relation, for all $i = 0, ..., N$,

$$\frac{\omega^2}{gd_ik_i^2} = \frac{\mathrm{sinc}(k_i\Delta_x)^2}{\frac{1}{3}(2+\cos(k_i\Delta_x))\left(\frac{1}{3}(2+\cos(k_i\Delta_x)) + \frac{1-\cos(k_i\Delta_x)}{\frac{k_i^2\Delta_x^2}{2}}\frac{k_i^2d_i^2}{3}\right)}, \tag{4.17}$$

whereas the terms of order of β provides the linear shoaling coefficients. Again, we obtain the relation between the amplitude U_i of the surface elevation and the bathymetry (see [5] for details). Finally for this numerical scheme,

$$\mathbf{A}_i = \frac{d_i}{\sqrt{gd_i}}\sqrt{1 + \frac{(1-\cos(k_i\Delta_x))}{\frac{k_i^2\Delta_x^2}{2}}\frac{1}{\frac{1}{3}(2+\cos(k_i\Delta_x))}\frac{k_i^2d_i^2}{3}}\mathbf{U}_i. \tag{4.18}$$

4.3. Analysis of the computations. In this section, we study the linear dispersion relations derived in Section 4.1 and 4.2. More precisely, we draw the phase velocity and the amplitude of the wave with respect to the dispersion parameter σ in shoaling conditions for each scheme and we compare the results with the ones predicted by the linear theory associated to the Peregrine equations (2.1).

4.3.1. Phase velocity. The phase velocity is usually given by the relation $C = \omega/k$. As observe in literature, we can consider k and d as constant functions ($k = k_0$, and $d = d_0$ see [27] for more details). Then, the phase velocity of our new numerical scheme (4.1)-(4.2) is given by (4.10) while that derived for the classical scheme (2.3)-(2.4) is given by (4.17). Our aim is to plot the two curves (4.10)-(4.17) and compare with the one predicted by the linear theory :

$$C_P^2 = \frac{gd}{1+\frac{k^2d^2}{3}}. \tag{4.19}$$

We first fix the wavelength λ and we put $\Delta_x = \frac{\lambda}{N_\lambda}$ where N_λ is the number of discretization points by wavelength. A direct computation gives $k\Delta_x = 2\pi/N_\lambda$. We recall that $\sigma = \frac{d}{\lambda}$, showing that $kd = 2\pi\sigma$. In Figure 2, we draw the relative errors between (4.2) and (4.17) and the phase velocity predicted by the linear theory. The error er is defined, for each scheme, by

$$\mathrm{er} = 100\left(\frac{C - C_P}{C_P}\right).$$

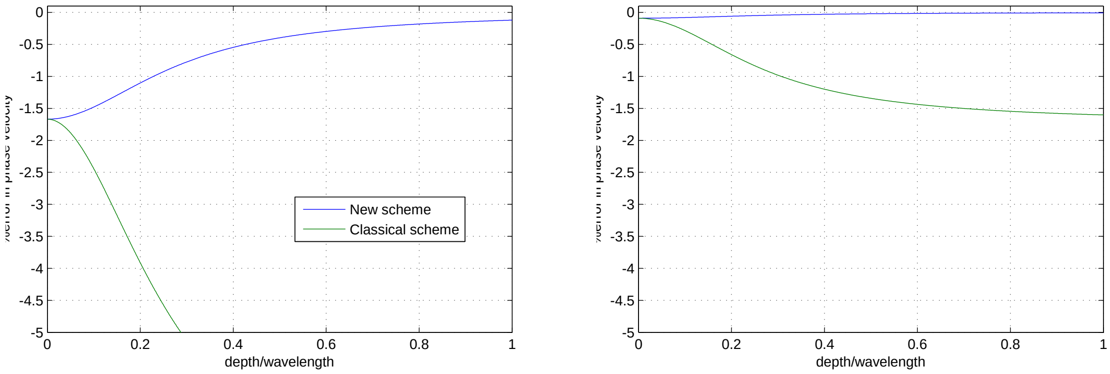

FIGURE 2. *Comparison of the phase velocity ($N_\lambda = 5$ on the left, $N_\lambda = 10$ on the right) of the classical and the new numerical scheme with the one given by the linear theory w.r.t σ.*

In Figure 2, one can observe that for $N_\lambda = 5$, the error coming from the new scheme is acceptable (less than 1.6%) whereas the one of the classical scheme is greater than 5% for depths bigger than 0.3. For $N_\lambda = 10$, although the error of the classical scheme is better than in the previous case (less than 2%), the one of the new scheme is much better and stay very close to 0. We conclude here that our new numerical scheme seems to reproduce much better the linear dispersive effects.

4.3.2. Linear shoaling test. We first recall the expression of the shoaling coefficients given by the linear theory associated with the Peregrine equations (2.1) (see [11]):

$$\alpha_1 = 2,\ \alpha_2 = 2 - \frac{k^2d^2}{3},\ \alpha_3 = 1,\ \alpha_4 = \frac{1}{2}\left(1 - \frac{k^2d^2}{3}\right),$$

and the expression of the surface elevation amplitude

$$A = \sqrt{1 + \frac{k^2d^2}{3}}\frac{d}{\sqrt{gd}}U. \tag{4.20}$$

Our aim is to compare, for a given situation, the evolution of the amplitude of the waves with respect to the space variable x given by the two relations (4.14) and (4.18) and the one derived from the linear theory. To this end, we perform the following test proposed by Madsen and Sorensen in [21]. We consider a periodic wave with an initial amplitude $a = 0.05$ and a wavelength $\lambda = 15$ starting from the position $x = 100$. It propagates over an initial constant water depth $d_0 = 13$. The bottom is flat until $x = 150$ and it has a constant up-slope of $\frac{1}{50}$ from $x = 150$ to $x = 790$. We compute the evolution of the wave amplitude with respect to x. For that, we propose the following procedure. Firstly, we integrate formally the relation between k and d ((4.12) for the new scheme), given by the differential equation

$$\frac{k'}{k} = -\alpha_4\frac{d'}{d}.$$

We use a Strongly Stability-Preserving Runge-Kutta method (SSP-RK) to compute the solution k, using $k_0 = \frac{2\pi}{\lambda}$ as initial condition. Then, we substitute this function k in the expression of α_s, and we compute the amplitude of the velocity U by integrating the relation

$$\frac{\mathbf{U}'}{\mathbf{U}} = -\alpha_s\frac{d'}{d}.$$

Again, we use a SSP-RK method and $\mathbf{U}(100) = a\frac{\sqrt{gd_0}}{d_0}$ as initial condition. Then, we deduce the theoretical amplitude of the wave elevation using Equations (4.14) (for the new scheme) and (4.18) (for the classical one). Fixing the value of Δ_x, it is possible to compute formally the surface elevation amplitude for each scheme. The results are presented in Figure 3.

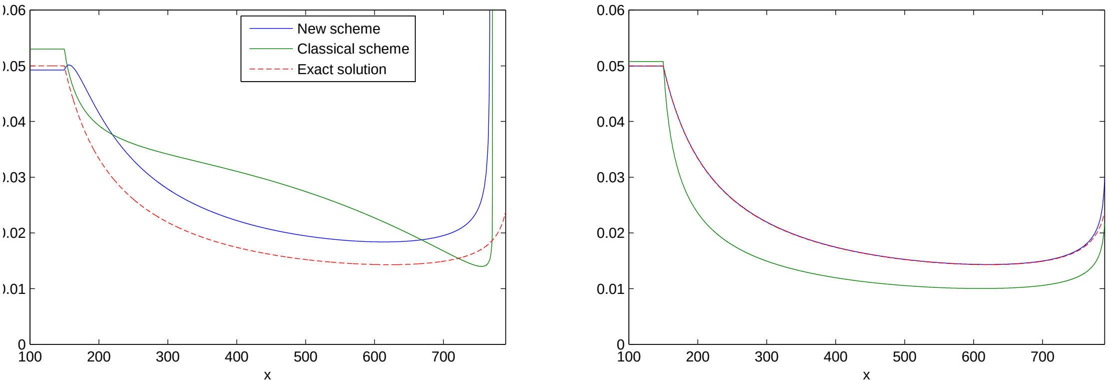

FIGURE 3. *Evolution of the wave amplitude for the two numerical schemes and for Peregrine equations. Left : $\Delta_x = 3$ ($N_\lambda = 5$). Right : $\Delta_x = 1.5$ ($N_\lambda = 10$).*

We observe that when Δ_x is small, the curves of the two schemes matched the theoretical one, meaning that both schemes converges. However, when Δ_x becomes larger, one can see that the curve computed with the new scheme stay closed to the theoretical one while the one computed with the classical scheme furnishes a bad behavior of the amplitude of the wave.

5. Numerical experiments. This section is devoted to the investigation of the behavior of the two schemes (3.51)-(3.52) and (2.3)-(2.4). To this end, we present different test cases : the propagation of solitary waves over a flat bathymetry, the propagation of a periodic wave on a flat bottom and on a constant slope. These test cases bring to the fore major differences between the two numerical models and confirms the preliminary results of Section 4. The choice of these test cases are motivated by the fact that it is an exact theory. But other tests highlight other characteristics. The interest reader can refer to [3], [17], [19] or [26].

5.1. Soliton propagation. We first consider the propagation of an exact solitary wave solution to the Peregrine equations, with an amplitude equal to 0.2 (details on the computation of this solution as well as mathematical conditions for the existence are given in [6]) over a flat bathymetry $d_0 = 1$. The space interval is equal to $[0, 200]$. In order to check our implementations, we have performed a grid convergence analysis. Numerical results have been compared with the initial profile (which is the profile of the exact solution). The meshes used contain respectively 1000, 2000, 4000 and 8000 points. In Figure 4, we have plotted the L^2-norm of the error for each scheme. The scheme (3.51)-(3.52) provide an error 3 or 5 times less important than that corresponding to (2.3)-(2.4). We deduce that with the same initial finite elements method, the new procedure decreases the error.

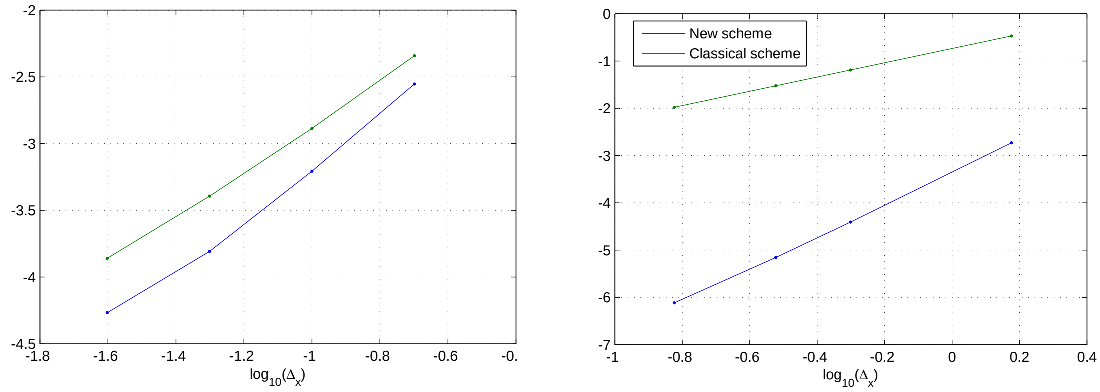

FIGURE 4. *Grid convergence results for a solitary wave propagating over a constant slope (on left) and of a periodic traveling wave (on right) for the two numerical schemes.*

5.2. Linear dispersion and linear shoaling test. In this section, we want to investigate the linear characteristics of the two numerical schemes. The idea is to confirm the study presented in section 4.

Firstly, we remark that there exist exact periodic traveling wave for the linear Peregrine equations with constant bathymetry. These solutions can be writing under the form:

$$\eta(t,x) = A\cos(k_0 x - \omega t),\ \bar{u}(t,x) = \frac{A}{d_0}\frac{\omega}{k_0}\cos(k_0 x - \omega t), \tag{5.1}$$

where $k_0 = 2\pi/\lambda$, A is the amplitude of η, and $\frac{\omega^2}{k_0^2} = \frac{g d_0}{1+\frac{k_0^2 d_0^2}{3}}$.

5.2.1. Linear dispersion test. The first test case consists in the propagation of an exact periodic traveling wave solution to the linear Peregrine equations, with an amplitude equal to 0.05 m over a flat bathymetry $d_0 = 13$ m and a wavelength $\lambda = 15$ m (then $\sigma = 0.87$). The space interval is equal to $[0, 150]$. We have performed computations for the two schemes with meshes containing 50 points (5 points per wavelength, and $\Delta_x = 3$), using periodic boundary conditions.

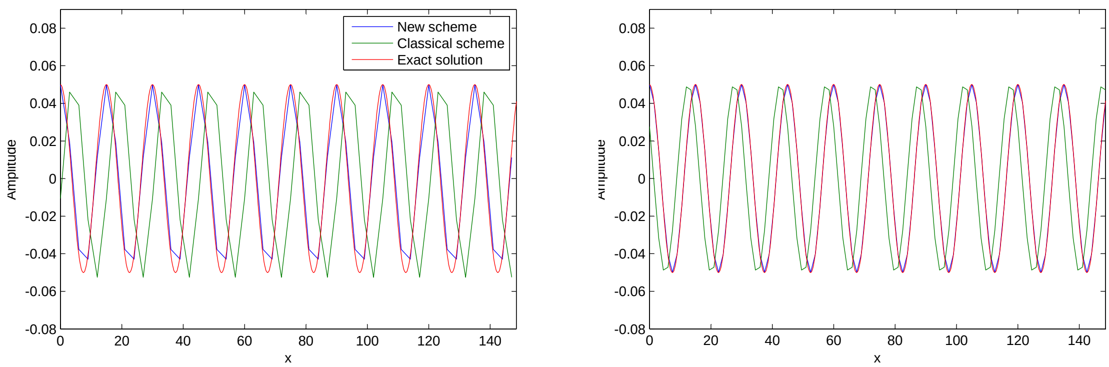

FIGURE 5. *Evolution of a traveling periodic wave for the two numerical schemes: Left :* $\Delta_x = 3$ *(*$N_\lambda = 5$*). Right :* $\Delta_x = 1.5$ *(*$N_\lambda = 10$*).*

In figure 5, we have plotted the results of the two schemes and the exact solution. One can observe a difference in the phase behavior of the two schemes. The solution computed with the new scheme (4.1)-(4.2) matches very well the reference curve, while the scheme (4.15)-(4.16) is shifted. Furthermore, for $N_\lambda = 5$, the green curves exhibits some small amplitude defects. But for $N_\lambda = 10$, one can observe that the classical scheme provides better results without reaching the precision of the other scheme. It confirms the results presented in figure 2. Finally, to compare the accuracy of the two models in these conditions, we have performed a grid convergence analysis. In Figure 4, we have plotted the error in the L^2-norm for each scheme, corresponding to successively 100, 300, 500 and 1000 points.

The slope obtained for the scheme (3.51)-(3.52) shows a convergence of order 3.4 while that corresponding to (2.3)-(2.4) is equal to 1.5. Furthermore, it is clear that the new model gives better results with 100 points that the classical scheme with 1000 points. We can deduce from this analysis that the new numerical scheme better reproduces linear dispersion effects.

5.2.2. Linear shoaling test. To further verify the results of section 4, we have performed the test case described in this section. Let us recall the procedure. A periodic wave of amplitude $A = 0.05$ m and wavelength $\lambda = 15$ m propagates over an initial constant bottom $d_0 = 13$. The periodic wave has been generated using a relaxation zone method [7]. The bottom is flat for the first 150 m , it has a constant slope of 1/50 from $x = 150$ m to $x = 800$ m. A wide absorbing sponge layers of 60 m long have been used at $x = 790$ m. The wave propagates during a time of 500 s, in order to stabilize the solution.

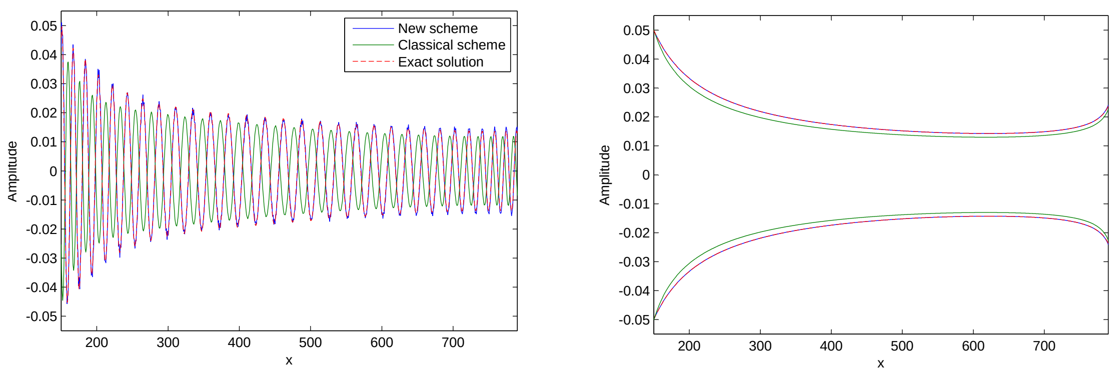

FIGURE 6. *Left: Shoaling wave profiles of Peregrine schemes* ($\Delta_x = 0.85$)*. Right: Theoretical envelope of the two numerical schemes* ($\Delta_x = 0.85$)*.*

Note that, to our knowledge, it is not possible to give an analytical solution in this configuration. We then decide to compute a reference solution using a very refined mesh of 10000 points ($\Delta_x = 0.085$) and the scheme (4.15)-(4.16). This solution is used as a standard in the sequel to make the comparisons. The conclusion doesn't changed if one computes the reference solution with the scheme (4.1)-(4.2).

In Figure 6, we have plotted the linear shoaling wave profile using a mesh containing 1000 ($\Delta_x = 0.85$) points for the two numerical schemes as well as the reference solution, and the theoretical envelope given by the analysis of the Section 4.3.2. Clearly, one can observe a major difference in the behavior of the two schemes. The solution emanating from the linear new scheme (4.1)-(4.2) matches very well the reference curve, showing that the convergence as already occurs with a few numbers of points while it is obviously not the case for the linear classical scheme (4.15)-(4.16). Indeed, the green curve exhibit some amplitude and phase defects. This test case confirms results given in Section 4, presented on Figure 6 on the right.

6. Conclusions and perspectives. We have presented a new systematic method to obtain discrete numerical model in the study of incompressible free surface flows. In order to evaluate the power of this method, we have considered the case of the so-called Peregrine equations and performed the computations in this academic situation. We have compared our new numerical scheme with the one obtained by performing directly a Galerkin method on the Peregrine equations. Finally, by the use of several numerical experiments, we have shown the efficiency of our new scheme to reproduce the linear effects although it is similar to the classical one in a nonlinear regime. Moreover, we claim that the method does not give a unique model. The choice of the initial scheme applied on Euler equations is an extra degree of freedom.
In the future, we plan to apply this new procedure to derive numerical schemes for Extended Boussinesq's models as well as for the Green-Naghdi equations. By this procedure, one of our goal is, for example, to enhance the linear dispersion characteristics of these models.

Acknowledgments. This study has been carried out with financial support from the French State, managed by the French National Research Agency (ANR) in the frame of the "Investments for the future" Programme IdEx Bordeaux - CPU (ANR-10-IDEX-03-02). Partial funding by the TANDEM contract (reference ANR-11-RSNR-0023-01 French *Programme Investissements d'Avenir*) is also acknowledged.

REFERENCES

[1] R. Abgrall and R. Saurel, Discrete equations for physical and numerical compressible multiphase mixtures. *Journal of Computational Physics*, 186 (2003), pp. 361-396.
[2] K. Adamy, Existence of solutions for a Boussinesq system on the half line and on a finite interval. *Discrete Contin. Dyn. Syst.*, 29 (2011), pp. 25-49.
[3] A. Ali et. al., Mechanical balance laws for Boussinesq models of surface water waves. *J. Nonlinear Sci.*, 22 (2012), pp. 371-398.
[4] S. Beji and K. Nadaoka, A formal derivation and numerical modeling of the improved Boussinesq equations for varying depth. *Ocean Engineering*, 23 (1996), pp. 691-704.
[5] S. Bellec, Sur des nouveaux modles asymptotiques en ocanographie. PhD University of Bordeaux, (2016).
[6] S. Bellec and M. Colin, On the existence of solitary waves for Boussinesq type equations and a new conservative model. Preprint.
[7] H.B. Bingham and Y. Agnon, A fourier-Boussinesq method for nonlinear water waves. *Eur. J. Mech. B/Fluids* 24 (2005), pp. 255-274.
[8] M. Bjørkavåg and H. Kalisch, Wave breaking in Boussinesq models for undular bores. *Phys. Lett.*, 275 (2011), pp. 1570-1578
[9] P. Bonneton, F. Chazel, D. Lannes, F. Marche and M. Tissier, A splitting approach for the fully nonlinear and wakly dispersive Green-Naghdi model. *Journal of Computational Physics*, 230 (2011), pp. 1479-1498.
[10] M. Brocchini, A reasoned overview on Boussinesq-type models: the interplay between physics, mathematics and numerics. *Proc. R. Soc. A*, 469 (2013).
[11] M.W. Dingemans, Water wave propagation over uneven bottoms. *Advanced Series Ocean Eng.*, (1997), World Scientific.
[12] A. Ern and J.-C. Guermond, Theory and practice of finite elements. *Applied Mathematical Sciences*, Vol. 159, Springer (2004).
[13] C. Eskilsson and S.J. Sherwin, Spectral/HP discontinuous Galerkin methods for modelling 2D Boussinsq equations. *Journal of Computational Physics*, 212 (2006), pp. 566-589.
[14] A. Filippini, S. Bellec, M. Colin and M. Ricchiuto, On the nonlinear behaviour of Boussinesq type models : amplitude-velocity vs amplitude-flux forms. *Coastal Engineering*, 99 (2014), pp. 109-123.
[15] S.T. Grilli, R. Subramanya, I.A. Svendsen and J. Veeramony, Shoaling of solitary waves on plane beaches. *J.Waterw.Port.C.-ASCE*, 120 (1994), pp. 609-628.
[16] M. Kazolea, A.I. Delis, I.K. Nikolos and C.E. Synolakis, An unstructured finite volume numerical scheme for extended 2D Boussinesq-type equations. *Coastal Engineering*, 69 (2012), pp. 42-66.
[17] Z. Khorsand et. al., On the shoaling of solitary waves in the KdV equation. *Proc. 34th Conf. Coastal Engrng.*, Seoul (2004).
[18] D. Lannes and P. Bonneton, Derivation of asymptotic two-dimensional time-dependent equations for surface water wave propagation. *Physics of fluids*, 21 (2009).

[19] M.S. Longuet-Higgins et. al., Radiation stresses in water waves; a physical discussion with applications. *Deep-sea Research*, 11 (1964), pp. 529-562.
[20] A. Madsen, R.Murray and O.R. Sorensen, A new form of the Boussinesq equations with improved linear dispersion characteristics. *Coastal Engineering*, 15 (1991), pp. 371-388.
[21] P.A.Madsen and O.R.Sorensen, A new form of the Boussinesq equations with improved dispersion characteristics. Part 2: a slowing varying bathymetry. *Coastal Engineering*, (1992), vol.18, pp. 183-204.
[22] D.E. Mitsotakis, Boussinesq systems in two space dimensions over a variable bottom for the generation and propagation of tsunami waves. *Mat. Comp. Simul.*, 80 (2009), pp. 860-873.
[23] O. Nwogu, Alternative form of Boussinesq equations for nearshore wave propagation. *ASCE Journal of Waterway, Port, Coastal and Ocean Engineering*, (1993), 618-638.
[24] D.H. Peregrine, Long waves on a beach. *J.Fluid.Mech*, 27 (1967), pp. 815-827.
[25] M. Ricchiuto and A.G. Filippini, Residual discretization of enhanced Boussinesq equations for wave propagation over complex bathymetries. *J. Comput. Phys.*, 271 (2014), pp. 306-341.
[26] I.A. Svendsen et. al., On the deformation of periodic long waves over a gently sloping bottom. *J. Fluid Mech.*, 87 (1978), pp. 433-448.
[27] M.K. Walkley, A Numerical Method for Extended Boussinesq Shallow-Water Wave Equations. PhD University of Leeds, (1999).
[28] M.A. Walkley and M. Berzins, A finite element method for the two-dimensional extended Boussinesq equations. *Int. J. Numer. Meth Fluids*, 39 (2002), pp. 865-885.